MODELLING PLASMA FLUORESCENCE INDUCED BY FEMTOSECOND PULSE PROPAGATION IN IONIZING GASES*

V. TOSA[1,2], A. BENDE[1], T. D. SILIPAS[1], H. T. KIM[2], C. H. NAM[2]

[1] National Institute for R&D of Isotopic and Molecular Technology, Cluj-Napoca, Romania
[2] Department of Physics, Korea Advanced Institute for Science and Technology, Daejeon, Korea

Received December 21, 2004

A three-dimensional (3D) nonadiabatic model for femtosecond pulse propagation in Ne gas was developed. The wave equation was solved by taking into account gas dispersion, optical Kerr effect and the presence of electron plasma due to ionization. The electron and laser intensity distribution in the interaction region are presented and compared with measurements of plasma fluorescence. Conditions for the occurrence of a self-guided propagation are discussed.

Key words: short intense laser pulse, propagation modelling, numerical model, self-guide propagation.

1. INTRODUCTION

The propagation of short, intense laser pulses in the atmosphere may have a number of important applications in the areas of active and passive remote sensing, electronic countermeasures, and induced electric discharges, artificial lightning. For example, localized ultraviolet radiation generated at a remote distance by laser ionization can provide a source for active fluorescence spectroscopy of biological and chemical agents in the atmosphere. Pulses of intense, directed white light may also find applications in the areas of hyperspectral imaging and differential absorption spectroscopy.

There is also a wide-ranging interest in understanding the channeled propagation process of femtosecond laser pulses through gaseous media. In 1996, Braun *et al.* [1] observed self-focusing into filaments in air with infrared laser pulses. The filaments can persist over several tens of meters. The mechanism for femtosecond laser pulses propagating over long distance in air is the balance between the Kerr self-focusing due to the nonlinear effects in air and defocusing due to the tunneling ionization and diffraction of the laser beam. Recently it was demonstrated [2] that self-guiding and flattening of the radial profile of the beam can take place not only as a balance between the positive

* Paper presented at the 5th International Balkan Workshop on Applied Physics, 5–7 July 2004, Constanța, Romania.

Rom. Journ. Phys., Vol. 50, Nos. 7–8, P. 741–748, Bucharest, 2005

Kerr contribution and negative plasma contribution to the refractive index, but, in a convergent beam, as a balance between the defocusing of the plasma of electrons and beam convergence. The initially spherical wavefront will be affected in its radius of curvature, more in the central and less in the peripheral regions along radial direction, so that it will flatten, propagating like a plane wave in the central part of the beam. This is of particular interest in high order harmonic generation where a uniform field, both in intensity and in phase, is desired over an extended part of the beam. Generation of the harmonics in these particular field configurations was proven [3, 4] to be highly efficient and with a good spatial and spectral characteristics.

The laser field in ionizing gas medium can be distorted by the modulation of refractive index which can vary in time and space. In space domain, a Gaussian beam (or any peaked laser beam) produces higher electron concentration in its central part than in the outer region, which results in the defocusing of laser field. On the other hand, the refractive index modulation induced by an electron concentration variation in time induces the self-phase modulation (SPM) of laser pulse. Since these two effects chiefly modify the pulse characteristics into unexpected one, control of ionization effects is an important issue in the investigation of the effects which the interaction between atoms and intense femtosecond laser pulses creates, such as high-order harmonics, self-channeling in air, and laser assisted particle acceleration.

2. NUMERICAL MODEL

To investigate the laser pulse propagation in ionizing medium, we performed three-dimensional (3D) nonadiabatic simulations of laser pulse propagation, taking into account the refractive index and absorption of neutral atoms, optical Kerr effect, and the variation of refractive index with electron density. In an ionized gas pulse propagation is affected by diffraction, refraction, nonlinear self-focusing, ionization, and plasma defocusing. The pulse evolution in such media are described by the wave equation which can be written as:

$$\nabla^2 E_1(r,z,t) - \frac{1}{c^2}\frac{\partial^2 E_1(r,z,t)}{\partial t^2} = \frac{\omega^2}{c^2}(1-\eta_{eff}^2)E_1(r,z,t) \tag{1}$$

where $E_1(r, z, t)$ is the transverse electric field of the laser, of frequency ω. Radial symmetry is assumed, therefore cylindrical coordinates are used throughout. The effective refractive index of the medium can be written as

$$\eta_{eff}(r,z,t) = \eta_0 + \eta_2 I(r,z,t) - \frac{\omega_p^2(r,z,t)}{2\omega^2} \tag{2}$$

The first linear term $\eta_0 = 1 + \delta_1 + i\beta_1$ accounts for the refraction (δ_1) and absorption (β_1), while the second term describes a $\chi^{(3)}$ process depending on laser intensity I, and known as the optical Kerr effect. Finally the third term contains the plasma frequency $\omega_p = (4\pi e^2 n_e/m)^{1/2}$ and accounts for the presence of a density n_e of electrons (of mass m and charge e) per unit volume. It is known [1] that if diffraction, self focusing due to η_2, and defocusing due to plasma generation are properly balanced, a self guided optical beam can be formed and propagated over extended distances, *i.e.* many vacuum Rayleigh lengths. Keeping only the real terms in the refractive index, the propagation equation for $E_1(r, z, t)$ becomes

$$\nabla^2 E_1(r, z, t) - \frac{1}{c^2}\frac{\partial^2 E_1(r, z, t)}{\partial t^2} = k^2\left(\frac{\omega_p^2}{\omega^2} - 2(\delta_1 + \eta_2 I)\right)E_1(r, z, t) \tag{3}$$

The method adopted to solve this equation is described by Priori et al. and will only be mentioned briefly here. We write the equation in the moving frame, and, after performing the paraxial approximation, eliminate the temporal derivative by a Fourier transform, and obtain the equation:

$$\nabla^2 E_1(r, z, \omega) - \frac{2i\omega}{c}\frac{\partial E_1(r, z, \omega)}{\partial z} = \tilde{F}\left[k^2\left(\frac{\omega_p^2}{\omega^2} - 2(\delta_1 + \eta_2 I)\right)E_1(r, z, t)\right] \tag{4}$$

where $\tilde{F}$ is the Fourier transform operator acting on the temporal coordinate. We mention that Priori *et al.* [5] solved the same equation taking into account only for the electrons plasma term.

From the numerical point of view, the right hand side of Eq. (4) has both an implicit (through plasma frequency term and $\eta_2 I$ term) and an explicit dependence on E_1. For this reason, Eq. (4) was solved selfconsistently in every δz step as follows. After advancing the solution $E(r, z, \omega)$ by a Crank-Nicolson scheme, we calculated $E(r, z, t)$ by a back Fourier transform, thus evaluated again the right hand side term of Eq. (4), firstly in t domain and then in ω domain. Crank-Nicolson scheme was applied again on the same step δz and a new $E(r, z, \omega)$ solution was obtained. The iteration was repeated until the difference between the new and the old solution was under an imposed threshold.

The energy loss by the pulse during propagation is made up of two contributions: the photoionization term represented by β_1 and the energy consumed in ionization processes. By writing the energy balance for the ionization process we obtain the imaginary contribution to the refractive index as $\gamma = (n_0 I_p w\lambda)/4\pi I$, where n_0 is the atomic density, I_p the ionization potential,

and w the ionization rate for an average intensity I. The energy loss was estimated for each (r, z) point after every successful integration step, and the dumped field was used in the next integration step. Energy loss by inverse bremstrahlung (collisional absorption) was not considered here because the working gas pressure is low.

To start the calculations we used the *measured* energy E_{pulse} and duration τ_p of the pulse to calculate the peak intensity, $I_0 = E_{pulse}/(\pi w_0^2 \tau_p)$. A Gaussian distribution in time and space was considered for the laser beam; the beam waist was approximated as $w_0 = f\lambda/D$, where D is the diameter of the iris used to truncate the beam before focusing. By placing the interaction cell in a specific z_L position, the E_1 initial and boundary values, needed to start solving the propagation equation, were calculated. In order to avoid reflection effects from the boundaries, we set the integration region radius to be three to four times larger than the beam waist.

In modelling the fluorescence signal which was measured, the basic assumption we make is that the observed fluorescence originates from the ions, thus, its intensity is proportional to the local ion concentration. In addition, we assumed that the ion concentration is equal to the electron concentration $n_e(r, z, \tau_p)$ at the end of the laser pulse. These assumptions are true only if we neglect multiple (mainly double) ionization processes in the interaction region and assume full ionization efficiency in the electron-atom collisions. The agreement with experimental data suggests that, for a qualitative description of the fluorescence, the above assumptions can be made in the simulated experimental conditions.

As mentioned before, to obtain the fluorescence profiles along the propagation direction, the measured data were integrated in the transverse direction. As a result, the fluorescence signal $S(z)$ can be linked to the radialy integrated electron concentration,

$$S(z) \propto \int n_e(r, z, \tau_p) r \, \mathrm{d}r \tag{5}$$

over the interaction region. An unknown parameter is the gas distribution in the vicinity of the nozzle ends, but it will only influence the fluorescence signal for about 5 mm after the input pinhole. On no physical grounds but solely to fit the data, we used the rational function $y = 1.1x/(0.1 + x)$, with x in mm, to describe the gas distribution for this region. For the rest of the cell the density was assumed to be constant.

To model the behaviour of the individual atom in the strong field created by the intense laser pulse we need to know the ionization rates of Ar. Ultrafast ionization rates of Ar were recently measured [6] using a pump-probe technique. The ionization rates reported were used to build up an interpolating polynomial

from which the rates for a given instantaneous intensity could easily be calculated. The resulting rate values were found to be smaller but close to the ADK rates corrected for intensity with a 1.7 factor, as described by Augst *et al.* [7].

3. RESULTS AND DISCUSSION

Laser pulses of 27-fs duration and wavelength centered at 827 nm were focused using a spherical mirror ($f = 1.2$ m), reaching a peak laser intensity of 2×10^{15} W/cm^2, onto a long neon gas jet with a 9-mm slit nozzle, where the peak gas density was about 40 Torr. To characterize the laser propagation through the gas medium, visible plasma image and laser beam profile after the medium were recorded by charge-coupled device (CCD) detectors. When the center of the gas jet nozzle was positioned at the laser beam focus, the gas jet position was defined as $z = 0$.

We observed drastic changes in the laser propagation when the gas jet position was moved along the laser propagation direction. The visible plasma image was monitored from a transverse direction and the laser beam profile at the end of the medium was also obtained by imaging it on a CCD. Fig. 1 shows two visible images of the plasma column obtained at the gas jet positions $z = 0$ and –18 mm using laser pulses of 5 mJ energy. When the gas jet was positioned at $z = 0$, the plasma image was bright only for the first 2-mm section of the gas medium due to the plasma defocusing effect. As the gas jet was moved to a

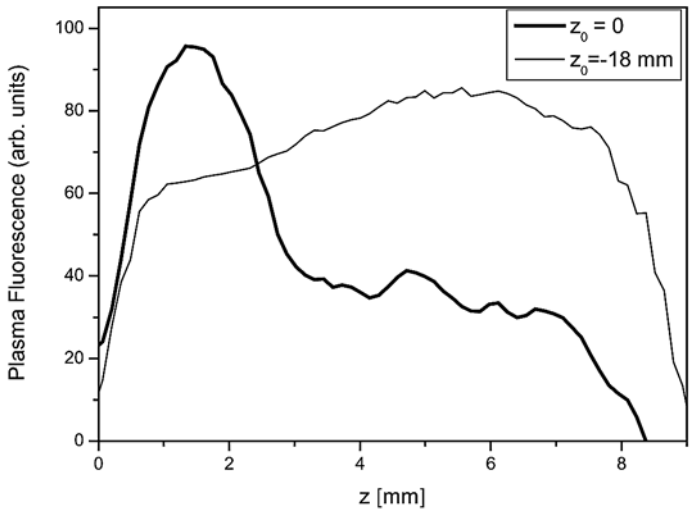

Fig. 1. – Fluorescence signal measured along the interaction region for two different positions of the cell with respect to the focus. Conditions described in the text.

position before the laser focus, the bright part of plasma image got extended and a nearly uniform plasma column was generated along the entire length of the gas jet when located at $z = -18$ mm. This shows clearly that the self-guiding of the propagating laser pulse occurs at properly selected target position.

The computed results are shown in Fig. 2 for different positions of the cell with respect to the focus. The behaviour observed in the experimental data could be fairly reproduced in the computed results. In particular, for the medium placed after the focus ($z_0 = 0$) the electron density exhibit a fast initial maximum followed by a rapid decrease. As the long jet position moves before the focus ($z_0 < 0$) the maximum of the electron concentration moves towards the middle of the region. This is in very good agreement with the trend observed in Fig. 1. The difference occurs in the position of the cell for which a particular distribution is formed. In the calculated data the distribution at $z_0 = -12$ mm corresponds to what was measured at $z_0 = -18$ mm. The reason is probably connected to the rate of ionisation which we used in the calculation. The beam spatial configuration and its departure from the calculated configuration of a truncated focused gaussian beam can also have an influence.

It is interesting to see, at this point, the intensity distributions which produced the electron distribution in the interaction region, for the two cases, namely $z_0 = 0$ and $z_0 = -12$ mm, because these kind of data help us to explain the fluorescence data. Fig. 3 contains 3D plots of the intensity distribution for the two cases. As one can see, the strong defocusing induced by the electron plasma

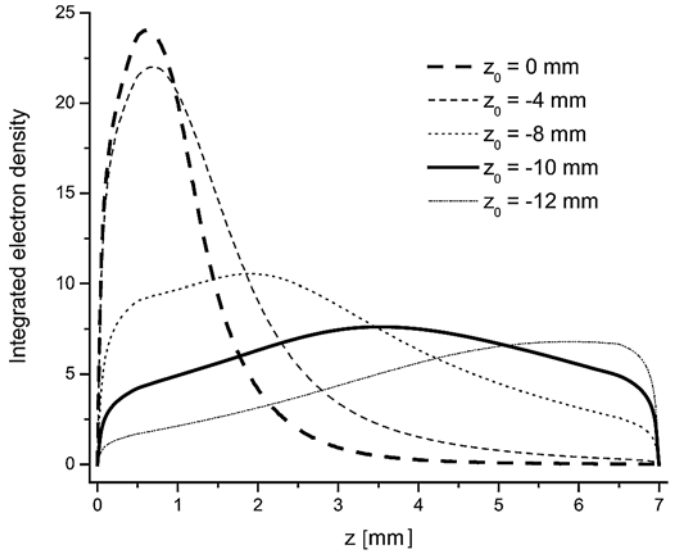

Fig. 2. – Computed electron density as a function of the axial coordinate, for different positions of the gas medium.

for $z_0 = 0$ case, will produce a strong and continuous decrease of the intensity, giving an overall configuration which is not favourable for high harmonic generation. On the contrary, the $z_0 = -12$ mm case produce, after an initial decrease, a region of constant intensity, in both axial and radial directions which extend for the whole interaction region. As demonstrated recently [2–4], this kind of configuration is particularly favorable for high order harmonic generation as it creates a large volume with a god phase matching characteristics.

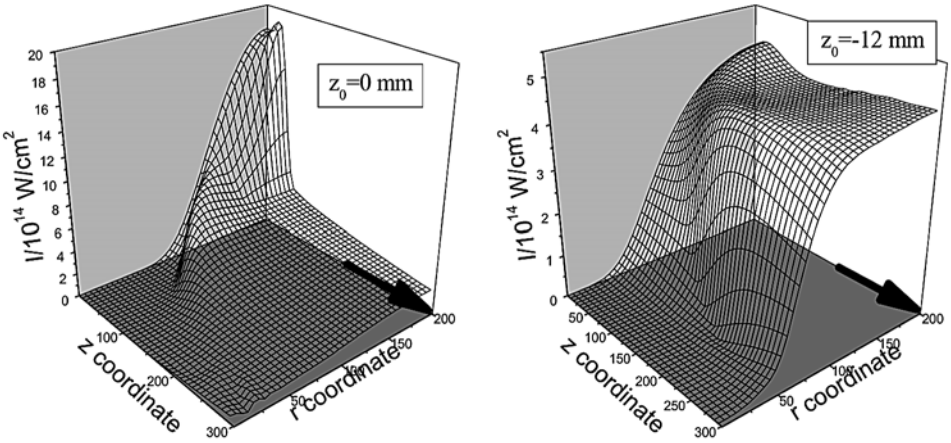

Fig. 3. – Laser intensity distribution in the interaction region for $z_0 = 0$ and $z_0 = -12$ mm.

As shown in [2] this self-guiding is different from the usual balancing between Kerr focusing and plasma defocusing, because in our range of pressures and field intensities, the Kerr contribution to the refractive index is small compared to that given by the electrons. In both cases, the electron plasma acts as a diverging lens with decreasing focal power as r increases. However, while in the first case the divergence of the beam is accentuated by the plasma, in the second case, the initial convergence of the beam tends to compensate the plasma divergent lens. As distinct from the common self-guiding effect, where the field confinement is due to the total internal reflection at the guide boundaries, in this case the effect is obtained due to a strong reflection of the trapped wave from the plasma boundary that is sharp as compared to the transverse scale. Indeed, one can easily imagine that the electron concentration in the interaction region follows closely the intensity distribution, shown in Fig. 3. The electron concentration will in turn affect the refractive index. Inside the self-guiding region the index is slightly less than unity while outside, where electron concentration sharply vanish, the index is greater than unity, due to neutral atoms contribution. In radial direction, the gradient of the refractive index, if over a given threshold [3] can act as a guide for the electromagnetic wave.

In conclusion, we presented experimental and calculated results concerning the propagation of a ultrashort laser beam in a gaseous medium. The formation of the self-guided beam, without Kerr self-focusing, was evidenced experimentally by measuring the plasma fluorescence in axial direction and confirmed by a 3D propagation model. Inside the self beam the pulse propagate like a plane wave in a confined cylinder. Finally, we mention that the self-guided propagation was confirmed also by measuring and modelling the transverse plasma profile [3], or by direct measurement of the near field [4] in the interaction region.

REFERENCES

1. A. Braun, G. Korn, X. Liu, D. Du, J. Squier, and G. Mourou, Opt. Lett. **20**, 73 (1995).
2. V. Tosa, E. Takahashi, Y. Nabekawa, and K. Midorikawa, Phys. Rev. A **67**, 063817 (2003).
3. E. Takahashi, V. Tosa, Y. Nabekawa, and K. Midorikawa, Phys. Rev. A **68**, 023808 (2003).
4. H. T. Kim, I. J. Kim, D. G. Lee, K. H. Hong, Y. S. Lee, V. Tosa, and C. H. Nam, Phys. Rev. A **69**, 031805 (2004).
5. E. Priori, G. Cerullo, M. Nisoli, S. D. Silvestri, P. Villoresi, L. Poletto, P. Ceccherini, C. Altucci, R. Bruzzese, and C. de Lisio, Phys. Rev. A **61**, 063801 (2000).
6. C. Siders, G. Rodriguez, J. Siders, F. Omenetto, and A. Taylor, Phys. Rev. Lett. **87**, 263002 (2001).
7. S. Augst, D. Meyerhofer, D. Strickland, and S. Chin, J. Opt. Soc. Am. B **8**, 858 (1991).